

Experimental confirmation of a new method for selective neutron separation^{*}

Yuri V. Drobyshevsky¹, Ilya M. Anfimov², Valery A. Varlachev³,
Svetlana P. Kobeleva², Sergey A. Nekrasov⁴, Sergey N. Stolbov¹

1 LLC Protius, 2 Proezd 4922, 124498 Zelenograd, Moscow, Russia

2 National University of Science and Technology MISIS, 4 Leninsky Ave., 119049 Moscow, Russia

3 National Research Tomsk Polytechnic University, 30 Lenin Ave., 634034 Tomsk, Russia

4 Central Economics and Mathematics Institute, RAS, 47 Nakhimov Ave., 117418 Moscow, Russia

Corresponding author: Sergey N. Stolbov (stolbovsn@mail.ru)

Academic editor: Georgy Tikhomirov ♦ **Received** 17 June 2020 ♦ **Accepted** 13 October 2020 ♦ **Published** 18 November 2020

Citation: Drobyshevsky YuV, Anfimov IM, Varlachev VA, Kobeleva SP, Nekrasov SA, Stolbov SN (2020) Experimental confirmation of a new method for selective neutron separation. Nuclear Energy and Technology 6(4): 235–241. <https://doi.org/10.3897/nucet.6.60294>

Abstract

The article presents an experimental confirmation of the operability of neutron concentrators in devices that form and use directed high-intensity thermal neutron beams with elliptical channels made as blocks of profiled graphite and aluminum plates. The effect of neutron reflection from the surface of materials is the basis of a device capable of selecting neutrons by their directions in space. The study experimentally confirmed the efficiency of a moderating-focusing structure (MFS) based on a pack of elliptical neutron mirrors, which makes it possible to form oriented thermal neutron beams from the outgoing neutron flux. To record the effects of selective thermal neutron separation, silicon single-crystal wafers were used, due to which it was possible to obtain portraits of integral neutron fluxes in the reactor. The experiments were carried out in a horizontal experimental channel (HEC-4) at the IRT-T reactor of the National Research Tomsk Polytechnic University. The integral neutron flux was $(2.3\text{--}3.02) \cdot 10^{17} \text{ cm}^{-2}$. The neutron flux was detected by the change in the specific electrical resistivity of the single-crystal silicon wafers. The effect of concentration of thermal neutrons was recorded both on the block of graphite neutron mirrors and on the block of aluminum thin-walled elliptical mirrors. In the near future, on this basis, it will be possible to solve such problems as extending the reactor life by reducing the hydrogen uptake in the inner walls. In addition, the experiments have proved the possibility of creating anisotropic structures that lie outside the formalism of Liouville's theorem, in which the surfaces of thermal neutron sinks are formed with subsequent concentration in the areas separated by aluminum or graphite plates.

Keywords

Thermal neutrons, neutron flux density, thermal neutron beams, elliptical mirror, method and apparatus for investigation thermal neutron beams, neutron transmutation, silicon

Introduction

One of the urgent tasks of modern science and technology is the creation of devices that form and use directed

high-intensity thermal neutron beams (Kim et al. 2017, Lehmann et al. 2017, Boffy et al. 2017). Such devices have a wide range of applications, for example, they open the way to the development of highly efficient neutron

* Russian text published: Izvestiya vuzov. Yadernaya Energetika (ISSN 0204-3327), 2020, n. 3, pp. 148–159.

detectors – a new technology for neutron transmutation doping of semiconductors (Varlachev et al. 1998, Varlachev and Solodovnikov 2009).

The possibility of implementing such devices is due to the fact that the neutron behaviors in the moderator, outside the moderator, and at the interface between the media are significantly different. The design of devices capable of selecting neutrons by their directions in space is based on the effect of neutron reflection from the surface of materials (Drobyshevsky and Stolbov 1990).

The angle of total external reflection of neutrons $j_s \approx \arcsin(u_{\text{bound}}/u_0)$ determined by the ratio of the boundary neutron speed u_{bound} on the surface of the substance to the speed $u_0 = 2200$ m/s of thermal neutrons of the reactor.

The j_s value is 10ϕ for the graphite surface, 12ϕ for beryllium, 10.7ϕ for iron, 11.5ϕ for nickel, 9.5ϕ for copper, and 5.0ϕ for aluminum (Drobyshevsky and Stolbov 1990).

We can represent the conditions for neutron reflection through the refractive index of neutrons on the surface of the substance as

$$n^2 = 1 - \frac{\lambda^2}{\pi} Nb \pm \frac{\mu_n B}{E_n}, \quad (1)$$

where $l = h/\mu_{\text{nn}}$ is the de Broglie wavelength of a neutron with a speed v_n ; N is the concentration of nuclei; b is the length of coherent scattering of matter nuclei; μ_n is the neutron magnetic moment; B is the magnetic induction of the field influencing the neutron inside the ferromagnetic; and E_n is the neutron energy.

The RF patent (Drobyshevsky and Stolbov 1990) proposes a design of a moderating-focusing structure (MFS) based on a pack of elliptical neutron mirrors, which makes it possible to form oriented thermal neutron beams from the outgoing neutron flux (Drobyshevsky and Stolbov 1990).

The aim of this work is to experimentally check the effect of selective neutron separation on individual plates on a block of selective elements.

To record the effects of selective thermal neutron separation, silicon single-crystal wafers were used, due to which it was possible to obtain portraits of integral neutron fluxes in the reactor.

The silicon single-crystal wafers were located near the pack of plates of the selective elements irradiated by the thermal neutron field of the reactor.

During irradiation of the silicon isotope ^{30}Si with neutrons, a stable isotope ^{31}P , is formed, neutron transmutation doping of silicon occurs (Varlachev et al. 1998) and its conductivity changes. The control is carried out by measuring the specific electrical resistance (SER) on the surface of the silicon single-crystal wafers. These wafers are convenient sensors for the reactor neutron flux due to the small cross-section of interaction between silicon and neutrons, which makes it possible to measure standard thermal neutron fluxes with acceptable accuracy.

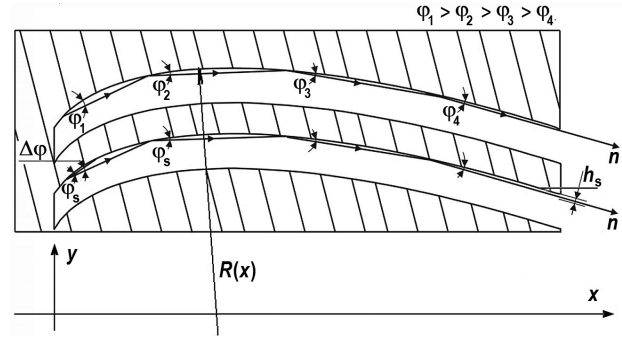


Figure 1. Selecting neutrons in curved selection channels: ϕ_1 is the angle of incidence-reflection of the neutron to the surface at $i-1$ -reflection; $\phi_2 \leq \phi_s$; ϕ_1 is the angle to the surface of the selection element for the primary entrance of the neutron n ; $\Delta\phi = \phi_1 - \phi_s$; h_s is the thickness of the near-wall layer of the selected flux; $R(x)$ is the radius of curvature of the selection element surface.

Design and operation of the moderating-focusing structure (MFS)

Let us consider multiple reflections of a near-wall thermal neutron flux on a profiled mirror with a variable, decreasing curvature along its motion. The separation of neutrons in curved selection channels is shown in Fig. 1.

The result of multiple reflection of near-wall neutrons on the surface of the plates, the radius of curvature R of which smoothly increases before each subsequent reflection of the beam, is that the near-wall concentration (compression) of the beam occurs.

The effect is realized for trajectories that start at any point on the surface during the formation of a chain of neutron beam reflections. Thus, the entire surface of a channel profiled in this way behaves as a continuous surface of sinks in the phase (angular) space of the diffuse neutron field. This set of sinks on the surface integrates the captured neutrons of the diffuse field and removes them in the direction selected by the curvature of the surface, while concentrating and increasing their phase density. Selective neutron capture occurs along its entire profiled surface, and extraction occurs on a narrow, $h_s \approx 5$ microns, strip at the end (with a well-polished surface). Therefore, the flux density along this strip can be high.

If the angle of surface reflection of neutrons is ϕ_s , the radius of curvature of the surface is R , the path of neutrons between reflections is $L_s \approx 2R \sin(\phi_s) \approx 5$ mm, and the distance of the trajectory from the channel surface is $h_s \approx R(1 - \cos(\phi_s))$, then the neutron capture efficiency during selection will be

$$K_{\text{sel}} = \frac{2R'_x}{\sqrt{1 - y_x'^2}}, \quad (2)$$

where y'_x is the derivative of the change in the coordinate of a point on the surface of the plate along x ; R'_x is the

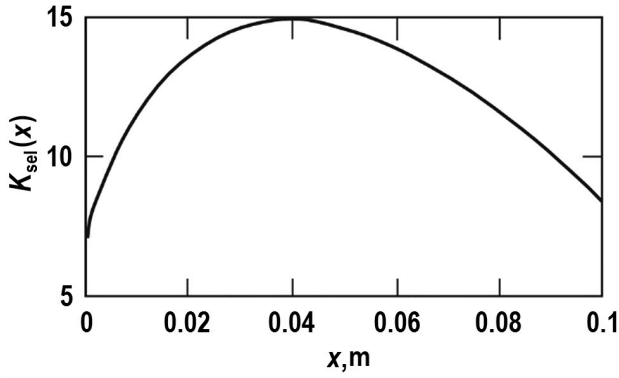


Figure 2. Selection efficiency on the surface of a selective element along its length.

derivative of the radius of curvature R of this surface with respect to x at this point.

The change in the selection efficiency K_{sel} of the surface of an selective element along its length is shown in Fig. 2.

For implementation, it is necessary to choose a geometry of the selective element surface with the maximum K_{sel} value on its most part. For example, for an element with an ellipse profile $x^2/a^2 + y^2/b^2 = 1$ with $a = 150$ mm, $b = 15$ mm, the maximum neutron selection efficiency $K_{sel} = 15$ is in the length range from 5 to 100 mm. For thermal neutrons to be selected with the entire volume of the structure, it is necessary that the following relation be fulfilled

$$N_s = \frac{\sigma_s}{\sigma_a} \geq \frac{2\pi}{K_{sel}\varphi_s} \frac{\pi}{\omega}, \quad (3)$$

where σ_s and σ_a are the neutron scattering and absorption cross-sections; N_s is the number of successive thermal neutron scatterings by the nuclei of matter before absorption; ω is the angle of divergence of the selected flux along the selection plane.

However, a thermal neutron lives for a rather long time in matter, constantly rescattering by its nuclei. The number of successive neutron scatterings by the nuclei of the moderator material is determined by the ratio of the cross-section for neutron scattering by a nucleus to the cross-section for its absorption by this nucleus, for example, for graphite $N_s = 1.3 \cdot 10^3$ times. For the pack of graphite plates (Varlachev et al. 1998)

$$N_s = 1.3 \cdot 10^3 \geq \frac{2\pi}{K_{sel}\varphi_s 0.5} \approx 300. \quad (4)$$

The MFS should have dimensions greater than the length of neutron diffusion in it.

In the limit, a thermal neutron can be selected by the structure in a preferred direction and pass through its focal region during its lifetime up to $1.3 \cdot 10^3 / 300 \approx 4$ times.

Or it can be said that the Q-factor (or technological albedo) of the MFS made of graphite is greater than unity and can reach 4.

Note that such a selection effect is possible only in the MFS for neutrons, since thermal neutrons of the diffuse



Figure 3. Appearance of the graphite selection plate in the first experiment.

field in the device repeatedly pass through the surfaces of the selective plate (an selective element) pack and are selected in it.

Unlike, for example, a photon of a diffuse scattered light source, a thermal neutron in such a transparent structure will have only one attempt to pass through the plates into the angular region of light photon capture by the structure and exit directionally. The effect will take place, the brightness of the formed narrow strip will increase, but the Q-factor of the device will be low.

Experiments and analysis

Three experiments were carried out to check the effect of selective neutron separation on profiled plates (Anfimov et al. 2018a, b). In the first experiment, 4 separated selection plates were made of graphite, and silicon detection wafers were placed across the neutron flux they formed. In the second and third experiments, the selection plates were made of aluminum, assembled in a pack, and the detecting silicon wafers (two in the second experiment and one in the third experiment) were placed along the neutron flux they formed in order to analyze their angular divergence. The experiments were carried out in a horizontal experimental channel (HEC-4) at the IRT-T reactor of the National Research Tomsk Polytechnic University (Anfimov et al. 2018a, b, Drobyshevsky et al. 2017).

The reactor is a pool-type VVER reactor with a capacity of 6 MW with beryllium as a moderator. The thermal neutron flux density is $1.0 \cdot 10^{13} \text{ cm}^{-2}\text{s}^{-1}$, the spectral coefficient is 106. The integral neutron flux of the reactor in the first experiment was $\Phi_1 = 3.02 \cdot 10^{17} \text{ cm}^{-2}$ (Anfimov et al. 2018b), in the second experiment on a plate pack – $\Phi_2 = 2.9 \cdot 10^{17} \text{ cm}^{-2}$ and in the third experiment – $\Phi_3 = 2.3 \cdot 10^{17} \text{ cm}^{-2}$. The appearance of the graphite selection plate in the first experiment is shown in Fig. 3, and the pack of selective elements in the second and third experiments is shown in Fig. 4.

After irradiation in the reactor and the decrease in the induced activity, measurements of the silicon wafers were carried out at the Department of Semiconductor Electronics and Semiconductor Physics at the National



Figure 4. Appearance of the package of selective elements in the second and third experiments.

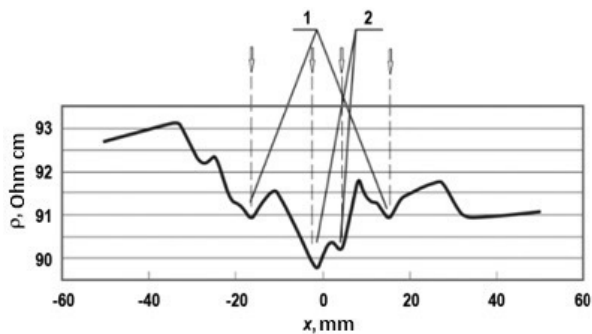


Figure 5. Profile of changes in the resistivity of silicon: 1 – the trace of neutron fluxes from the external selection plates with $K_{sel} = 10$; 2 – the trace of neutron fluxes from the internal selection plates with $K_{sel} = 15$. The vertical dashed lines with the arrows indicate the directions of the thermal neutron flux from the four graphite selection plates.

University of Science and Technology MISIS. The work was carried out on an automated installation for visual and measuring testing of the specific electrical resistivity (SER) of semiconductor materials by the four-probe method. In the first experiment, the following picture of the change in the resistivity of silicon on the trace of the neutron flux from four selection plates was obtained (Anfimov et al. 2018a).

Fig. 5 shows the resistivity profile of the plate from the first experiment.

The resistivity map was taken on the surface of the plates with a variable pitch in a cylindrical coordinate system. Due to the dependence between the absorbed integral dose on the thermal neutron flux and the conductivity of silicon, this is an effective method for measuring the reactor neutron field (Anfimov et al. 2018b). It was shown in the experiment that the increased conductivity bands of silicon (and, therefore, increased intensity of the neutron flux) are in those regions where the plates are located and the conductivity at the minima of the SER trace coincides with the calculated one.



Figure 6. Appearance of the detection discs (1) and the end of the pack of 20 selection plates (2) in the container in the second and third experiments.

In the second and third experiments, a pack of 20 aluminum plates was used. In this case, neutrons from the external diffuse field of the reactor are selected on the pack of selection plates. To record the effect in the second case, we used a pack of two silicon wafers 101.8 mm in diameter and 2.4 mm thick mounted with an edge along the direction of the neutron flux. In the third case, one 4 mm thick wafer was used. The selection plates were made of a rolled aluminum strip (A0 grade) 0.5 mm thick and 70 mm wide with a spacer flange along the edges, formed in such a way that the geometric focus in the direction of which the plates orient the selected neutrons is at a distance of 100 mm from the edge of the plates. The profile of the selection plates was chosen as a part of an ellipse, as it was done in the first experiment. Fig. 6 shows the detection plates from the side of the open end of the container.

Fig. 7 shows the map of the SER distribution in the third experiment.

The calculated SER value of the irradiated sections of the original silicon is related to the concentration of N_q -carriers generated by irradiation with the integral neutron flux Φ , by the relation $r_{exp} = (eN_q\mu_n)^{-1}$, where $e = 1.602 \cdot 10^{-19}$ C; $\mu_n \approx 1350$ cm²·V⁻¹·s⁻¹ is the electron mobility in silicon at the received radiation dose.

The expected specific electrical resistivity of silicon in the integral neutron flux of the reactor $\Phi = 3.02 \cdot 10^{17} \pm 3\%$ cm⁻² in the absence of the selection effect should have been about 96 Ohm·cm. This is usually reproduced in experiments with an average thermal neutron flux in the reactor of $1 \cdot 10^{13}$ cm⁻²·s with an accuracy of $\pm 3\%$.

The SER value on the irradiated silicon wafers turned out to be lower than it had been expected, which means

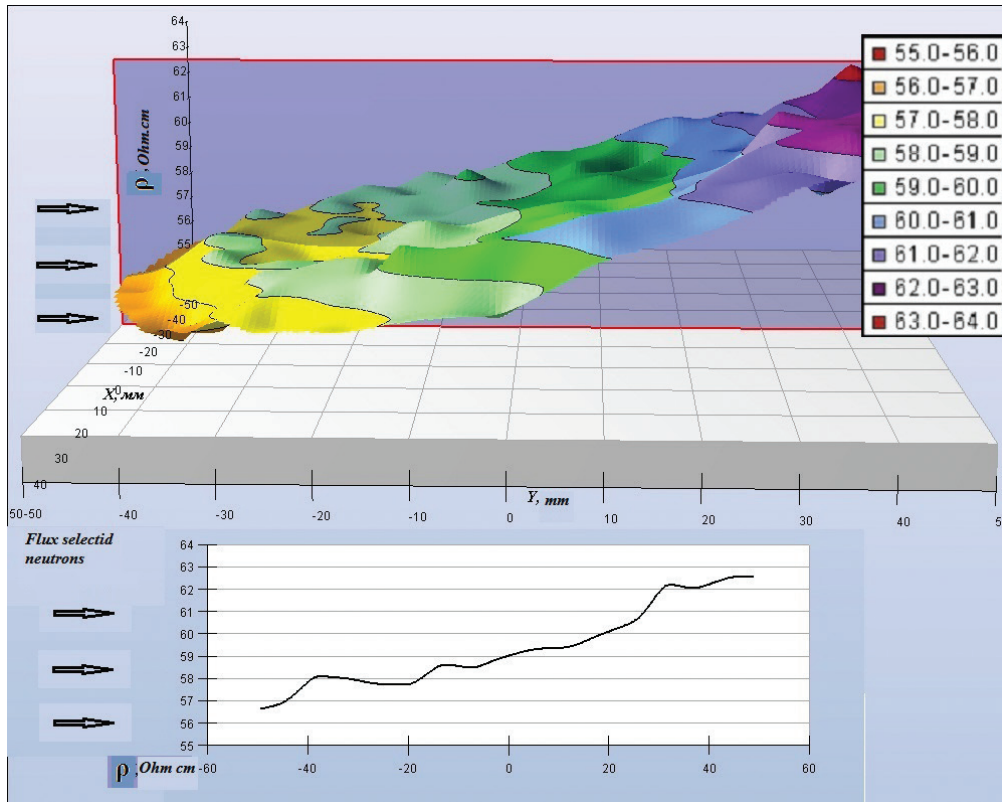


Figure 7. Map of SER changes along the control silicon wafer (top) and SER change along the control silicon wafer (bottom).

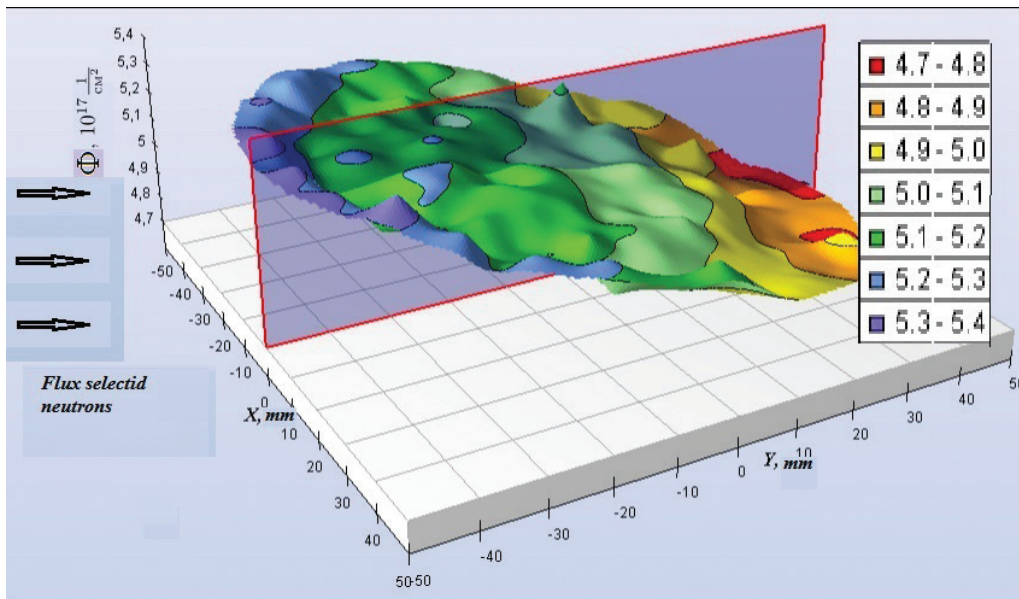


Figure 8. Change in the integral flux of thermal neutrons recorded on the control silicon wafer.

that the flux density of the thermal neutrons selected by the experimental block of elements of the selective structure turned out to be higher.

Based on the measurements of the conductivity of silicon, the integral of the flux of thermal neutrons recorded on its substance was restored. In this case

$$\Phi_{\text{exp}} = (e \cdot \rho_{\text{exp}} \cdot \mu_n \cdot n_{\text{Si}} \cdot \sigma_{\text{Si}30} \cdot 0.031)^{-3} \approx \frac{300 \cdot 10^{17}}{\rho_{\text{exp}}} \pm 3\% \left(\frac{1}{\text{cm}^2} \right) \quad (5)$$

where n_{Si} is the concentration of silicon in the wafer; 0.031 is the fraction of ^{30}Si in natural silicon; $\sigma_{\text{Si}30}$ is the cross-section for interaction of neutrons with ^{30}Si .

Fig. 8 shows a distribution map of the integral neutron flux.

It was found that the neutron flux on the wafer increased to a value of $\Phi = 5.3 \cdot 10^{17} \pm 3\% \text{ cm}^{-2}$ at an integral flux of the neutron field in the reactor $\Phi = 2.3 \cdot 10^{17} \pm 3\% \text{ cm}^{-2}$.

At least a twofold increase was shown in the integral flux of thermal neutrons due to the selective separation of neutrons on the pack of 20 selection elements. The sectorial block of profiled selection elements made of aluminum is 1/45 of the full cylinder and has a length of 70 mm along the axis. With a full-fledged cylindrical moderating-focusing structure, the thermal neutron flux would be 90 times greater than the thermal neutron flux of the reactor.

A fairly simple device was tested in which the density in the flux increases, but the angular divergence of the near-wall beam decreases. Formally, Liouville's theorem for beams is violated, which is often interpreted as the statement that "using optical devices: waveguides, lenses, mirrors of different shapes, it is impossible to increase the density in the phase space".

Liouville's theorem states that the phase volume (or probability density in phase space) is preserved in time. It follows from the equation of continuity with the missing term describing the divergence, which means that there are no sources or sinks of the probability density. In other words, Liouville's theorem (in particular, Liouville's theorem for beams) is formulated for the case of systems in which sources and sinks are excluded by boundary conditions.

But in the MFS, the surface of each profiled selection plate behaves like a continuous surface of sinks in the phase (angular) space of the diffuse field of thermal neutrons, which form the source of the directed flux at the end. And, therefore, the process for selective neutron separation lies outside the boundary conditions of Liouville's theorem.

Thus, there is no violation of Liouville's theorem. But at the same time, the experiments proved the possibility of creating anisotropic structures lying outside its formalism, in which the surfaces of thermal neutron sinks from the diffuse field of thermal neutrons are formed, with subsequent concentration in the regions separated by the structures.

As a result of the experiments, in nuclear technology an instrument appeared, which:

- firstly, in contrast to purely gradient control of neutron diffusion in a conventional reactor, efficiently controls thermal neutron fluxes, at the same time thermalizing fast neutrons and creating a directed flux from the diffuse field of thermal neutrons (Badretdinov et al. 2010, Solovyeva et al. 2019, Vatulin et al. 2015, Fischer et al. 2019, Zain et al. 2018, Thomas and Belle 2019); and
- secondly, due to the high efficiency of reflection of thermal neutrons from mirror surfaces, makes it possible to create a wide class of various devices for nuclear power engineering, experimental physics (Drobyshevsky et al. 2017) and controlled neutron transmutation doping of substances (Drobyshevsky et al. 2012, Badretdinov et al. 2010).

Conclusions

The effect of selective neutron separation was recorded on the selective elements made of graphite and on a block of profiled aluminum plates. The obtained experimental results can be used in a new generation of both nuclear and thermonuclear reactors for developing various devices with an increased thermal neutron flux density and high-performance neutron detectors as well as for creating new technologies for neutron transmutation doping of semiconductors, or in experimental physics. The results are of interest for various applications of dense neutron fluxes.

In particular, on their basis, it is possible to solve such problems as reducing the time of irradiation with a thermal neutron flux of experimental samples when they are placed in the focal regions of the MFS.

References

- Anfimov IM, Drobyshevsky YuV, Stolbov SN (2018a) Recording the Effect of Selective Thermal Neutron Separation. *Izvestia Instituta Inzhenernoy Fiziki* [Bulletin of the Institute of Engineering Physics], 3(49): 21–26. [in Russian]
- Anfimov IM, Varlachev VA, Drobyshevsky YuV (2018b) Recording the Effect of Selective Thermal Neutron Separation. *Voprosy atomnoy nauki i tekhniki. Seriya: Fizika radiatsionnogo vozdeystviya na radioelektronnuyu apparaturu* [Problems of Atomic Science and Technology. Series: Physics of Radiation Effects on Electronic Equipment] 1: 24–30. [in Russian]
- Badretdinov TH, Goryunov AG, Varlachev VA (2010) On the Issue of Upgrading the Complex of Neutron Transmutation Doping of Silicon at IRT-T. *Izvestia vuzov. Yadernaya energetika* [News of Higher Educational Institutions. Nuclear Power Engineering] 3: 147–151. [in Russian]
- Boffy R, Beaucour J, Bermejo FJ (2017) A Versatile Device for Thermal Neutron Irradiation of Materials at Grazing Incidence Angles. *Nuclear Technology* 200(1): 54–65. <https://doi.org/10.1080/00295450.2017.1341780>
- Drobyshevsky YuV, Dunilin VM, Volkov GG, Stolbov SN (2017) Reactor Neutrons, Neutron Structure and Space-Time Geometry. *Izvestia Instituta Inzhenernoy Fiziki* [Bulletin of the Institute of Engineering Physics] 3: 17–28. [in Russian]
- Drobyshevsky YuV, Stolbov SN (1990) *Ustroystvo dlya formirovaniya napravlennoy potoka neytronov* [Device for Forming a Directed Neutron Flux], Patent RU No.1821818. [in Russian]
- Drobyshevsky YuV, Stolbov SN, Nekrasov SA, Petrov GN, Prokhorov AK (2012) Method and Device for Neutron Transmutation Doping of a Substance. Patent RU No.2514943. [in Russian]
- Fischer V, Pagani L, Pickard L, Grant C, He J, Pantic E, Svoboda R, Ullmann J, Wang J (2019) Absolute Calibration of the DANCE Thermal Neutron Beam Using Sodium Activation. *Nuclear Instruments and Methods in Physics Research. Section A, Accelerators, Spectrometers, Detectors and Associated Equipment* 929(C): 97–100. <https://doi.org/10.1016/j.nima.2019.03.047>
- Kim YH, Park H, Kim YK, Kim J, Kang J (2017) Reference thermal neutron field at KRISS for calibration of neutron detectors. *Radiation Measurements* 107: 73–79. <https://doi.org/10.1016/j.radmeas.2017.10.001>

- Lehmann E, Trtik P, Ridikas D (2017) Status and perspectives of neutron imaging facilities, Neutron imaging for applications in industry and science. *Physics Procedia* 88: 140–147. <https://doi.org/10.1016/j.phpro.2017.06.019>
- Solovyeva AP, Ulyanin YuA, Kharitonov VV, Yurshina DYU (2019) On the Value of SNF as a Raw Fuel Material for Thermal Reactors. *Izvestia vuzov. Yadernaya energetika* [News of Higher Educational Institutions. Nuclear Power Engineering] 2: 140–152. [in Russian] <https://doi.org/10.26583/npe.2019.2.12>
- Kerlin TW, Upadhyaya BR (2019) Chapter 2 – Nuclear reactor designs. In: *Dynamics and Control of Nuclear Reactors*. Elsevier Science, Academic Press, 5–16. <https://doi.org/10.1016/B978-0-12-815261-4.00002-0>
- Varlachev VA, Solodovnikov ES (2009) A Thermal Neutron Detector Based on Single-Crystalline Silicon. *Instruments and Experimental Techniques* 52(3): 342–344. <https://doi.org/10.1134/S0020441209030063>
- Varlachev VA, Solodovnikov ES (2010) Improving the Efficiency of Using Neutrons with Uniform Irradiation of Large Samples. *Izvestiya vuzov. Fizika* [News of Higher Educational Institutions. Physics] 53(10–2): 313–316. [in Russian]
- Varlachev VA, Zenkov AG, Solodovnikov ES (1998) Features of Neutron-Transmutation Silicon Doping at Research Reactors. *Izvestiya vuzov. Fizika* [News of Higher Educational Institutions. Physics] 4: 210–215. [in Russian]
- Vatulin AV, Suprun VB, Kulakov GV (2015) Fabricating Fuel for Research Reactors. *Atomnaya Energia* [Nuclear Energy] 119(5): 249–254. [in Russian] <https://doi.org/10.1007/s10512-016-0064-4>
- Zain JAI, Hajjaji OEI, Bardouni TEL, Boukha H (2018) Deterministic Evaluation of Safety Parameters and Neutron Flux Spectra in the MNSR Research Reactor Using DRAGON-4 Code. *Journal of Radiation Research and Applied Sciences* 11(3): 255–261. <https://doi.org/10.1016/j.jrras.2018.04.002>